Search for Higgs Decay to Dark Matter and Trigger Studies

João Carlos Arnauth Pela
of Imperial College London

A dissertation submitted to Imperial College London
for the degree of Doctor of Philosophy

Abstract

Here the abstract of the thesis

Declaration

This dissertation is the result of my own work, except where explicit reference is made to the work of others, and has not been submitted for another qualification to this or any other university. This dissertation does not exceed the word limit for the respective Degree Committee.

João Pela

Acknowledgements

TODO:

- Family
- Friends
- Work colleagues (include CMS collaboration)
- more

The work presented in this thesis was supported by the Portuguese Government through Fundação para a Ciência e a Tecnologia (FCT) in the form of my PhD grant with the reference SFRH/BD/77979/2011. I am thankful for their support which allowed me to attain higher education.

Preface

Thesis structure and so on...

"To my grand mother"

Contents

1 Theory **2**

1.1 Standard Model of Particle Physics . . . 2
1.2 Higgs Mechanism . . . 3
1.3 Higgs Invisible decays . . . 3

2 Experimental Apparatus **4**

2.1 The Large Hadron Collider . . . 4
2.1.1 Running and performance . . . 8
2.2 The Compact Muon Solenoid Experiment . . . 9
2.2.1 Geometry and conventions . . . 11
2.2.2 Inner tracking system . . . 11
2.2.3 Electromagnetic Calorimeter . . . 12
2.2.4 Hadronic Calorimeter . . . 14
2.2.5 Solenoid Magnet . . . 16
2.2.6 Muon System . . . 17
2.2.7 Data Acquisition System . . . 19
2.2.8 Trigger System . . . 19
2.2.9 Computing . . . 21
2.2.10 Level 1 Trigger: Stage I Upgrade . . . 22

3 Technical work **23**

3.1 Level 1 Trigger Data Quality Monitoring System . . . 23

4 Physics Objects and Monte Carlo simulation **24**

4.1 Physics objects definition . . . 24
4.1.1 Electron . . . 24
4.1.2 Muon . . . 24
4.1.3 Tau . . . 24
4.1.4 Jets . . . 24

4.1.5 Missing Transverse Energy 24
4.2 Monte Carlo simulation 24

5 Prompt Data Analysis **25**

6 Parked Data Analysis **26**

7 Run II Preparation **27**
7.1 Run II trigger studies 27
7.2 Run II QCD Monte Carlo samples 27

8 Conclusions **28**

Bibliography **30**

List of Figures **32**

List of Tables **33**

Acronyms **34**

Chapter 1

Theory

TODO:
- Global status

1.1 Standard Model of Particle Physics

TODO:
- Very brief summary of the Standard Model.

The Standard Model (SM) of particle physics is the currently accepted model for describing the physics of elementary particles.

Leptons (J=1/2)				
Generation	Particle Name	Symbol	Mass (GeV/c^2)	Q/e
1^{st}	Electron	e	0.000511	1
	Electron Neutrino	ν_e	$< 3 \times 10^{-}9$	0
2^{nd}	Muon	μ	0.106	1
	Muon Neutrino	ν_μ	$< 1.9 \times 10^{-}4$	0
3^{rd}	Tau	τ	1.777	1
	Tau Neutrino	ν_τ	$< 1.82 \times 10^{-}2$	0

Table 1.1: List of leptons and their fundamental properties

Quarks (J=1/2)				
Generation	Particle Name	Symbol	Mass (GeV/c^2)	Q/e
1^{st}	Up	u	$1.5 - 3.3 \times 10^{-3}$	-2/3
	Down	d	$3.5 - 6 \times 10^{-3}$	1/3
2^{nd}	Charm	c	1.16-1.34	-2/3
	Strange	s	$70 - 130 \times 10^{-3}$	1/3
3^{rd}	Top	t	169-173	-2/3
	Bottom	b	4.13 – 4.37	1/3

Table 1.2: List of quarks and their fundamental properties

Bosons			
Particle Name	Mass (GeV/c^2)	Q/e	Spin
Photon (γ)	0	0	1
$W^{\pm}$	80.4	∓ 1	1
Z^0	91.2	0	1
Gloun (g)	0	0	1
Higgs (H^0)	> 114	0	0

Table 1.3: List of bosons and their fundamental properties

1.2 Higgs Mechanism

Summary of the Higgs Mechanism. Should include

- Motivations
- Explanation of the mechanism itself
- Consequences
- Possible decays

1.3 Higgs Invisible decays

TODO:

- Explain what are SM Higgs invisible decays.
- Go over the possibility of BSM invisible decays.

Chapter 2

Experimental Apparatus

2.1 The Large Hadron Collider

The Large Hadron Collider (LHC)[1] is currently the world's largest particle accelerator and is capable to produce the highest energy particle beams ever made by mankind. This gigantic machine with a total perimeter of 26.7 km was built at European Organization for Nuclear Research (CERN) in a circular tunnel, where previously the Large Electron Positron collider (LEP)[2] was installed, at an average depth of 100 m below ground under the Franco-Swiss border near Geneva, Switzerland. A diagram of the LHC tunnel and its experiments can be found at figure 2.1.

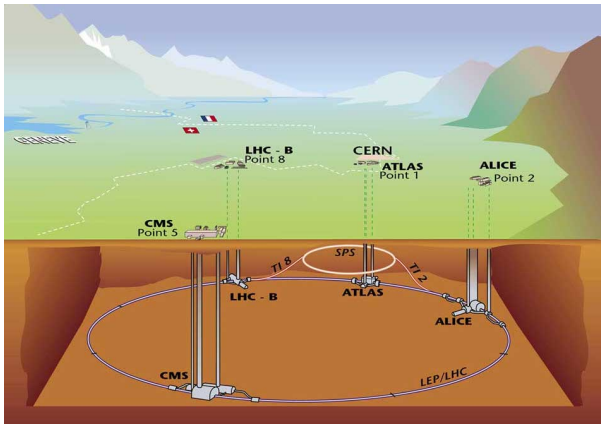

Figure 2.1: Underground diagram of the Geneva area showing the LHC and its experiments location.

The LHC is a synchrotron machine with the capability to accelerate two particles beams in opposite directions in two separated beam pipes. These beams only cross and are forced to collide in four points of the accelerator where huge particle detectors are installed to

detect the products of such collisions. This experiments are: A Toroidal LHC ApparatuS (ATLAS)[3], Compact Muon Solenoid (CMS)[4], Large Hadron Collider beauty (LHCb)[5] and A Large Ion Collider Experiment (ALICE)[6].

The objective of the LHC program is to investigate physics at the TeV scale, more specifically to understand the electroweak symmetry breaking and if this phenomena could be explained by the Higgs mechanism. There are many Beyond the Standard Model (BSM) models that predict new physics at this energy regime making the LHC the perfect machine to investigate such phenomena. ATLAS and CMS are general-purpose detectors which aim to investigate a broad spectrum of physics. The LHCb detector is used to study processes that involve the decay of b-flavoured hadrons. The ALICE detector is optimised to look at heavy-ion collisions and to investigate the properties of extreme high density medium that is formed.

The LHC is only the last element of a complex accelerator chain which step-by-step increases the energy of the particles to eventually be collided. Protons are initially obtained by stripping the electrons of hydrogen gas. This process happens at the begging of the Linear Particle Accelerator 2 (LINAC2) which then accelerates them up to the energy of 50 MeV. After this initial step proton are injected into the Proton Synchrotron Booster (PSB) and the energy ramps ups to 1.4 GeV. Particles are then passed to the Proton Synchrotron (PS) where the energy futher increases to 25 GeV. Subsequently they are the injected into the Super Proton Synchrotron (SPS) where the particle energy level reaches 450 GeV. Finally, protons pass to the LHC where they can be accelerated to a maximum energy of 7 TeV. A simplified diagram of the CERN accelerator chain can be found in figure 2.2. Normal operation of the LHC therefore depends on all the upstream accelerators availability. The typically turn around time, the time necessary to stop the accelerator from running and restart collisions, is around 2 hours. When stable beams are achieved, a single proton fill can be used to collide protons up to 24 hours, but it is common to restart more frequently to take profit of the higher collision rates possible right at the beginning of a new fill.

The LHC as its name indicates can collide hadrons, more specifically proton or heavy ions. Three modes of operation have been tried according to the particles used: proton-proton, proton-lead and lead-lead. By changing the incoming particles we are changing the quantity of nucleons present at each interaction. The maximum design energy per proton is 7 TeV and for each lead nucleon 2.76 TeV. The maximum design luminosity for proton-proton is of $10^{34}\,\mathrm{cm}^{-2}\mathrm{s}^{-1}$ and for lead-lead is of $10^{27}\,\mathrm{cm}^{-2}\mathrm{s}^{-1}$.

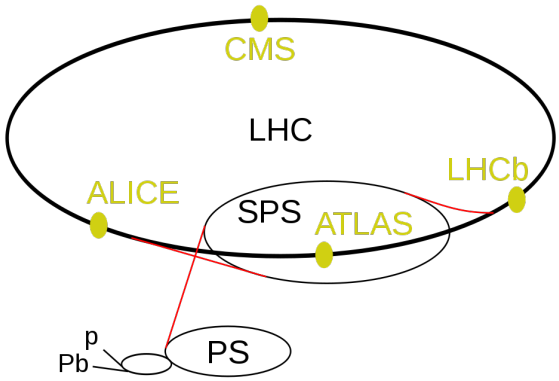

Figure 2.2: Diagram of the CERN accelerator complex.

Particles beams trajectory are curved by 1232 niobium-titanium superconducting dipole magnets each with a length of 14.3 m, they are cooled with superfluid helium to 1.9 K to be able to produce the necessay magnetic field of 8.4 T. To accelerate the beam eight Radio Frequency (RF) cavities located at the LHC point 4 are used. At each turn particle energy is increased to compensate for synchrotron radiation loss and increase the momentum. At nominal operation the LHC will steer 2808 bunches separated by 25 ns in each direction each bunch is composed up to 10^{11} protons. Some of the key parameters of the LHC proton-proton and lead-lead operation can be found in table 2.1.

		pp	**HI**	
Energy per nucleon	E	7	2.76	TeV
Dipole field at 7 TeV	B	8.33	8.33	T
Design Luminosity*	$\mathcal{L}$	10^{34}	10^{27}	$\mathrm{cm}^{-2}\mathrm{s}^{-1}$
Bunch separation		25	100	ns
No. of bunches	k_B	2808	592	
No. particles per bunch	N_p	1.15×10^{11}	7.0×10^{7}	
Collisions				
β-value at IP	β^*	0.55	0.5	m
RMS beam radius at IP	σ^*	16.7	15.9	µm
Luminosity lifetime	τ_L	15	6	h
Number of collisions/crossing	n_c	≈ 20	-	

* For heavy-ion (HI) operation the design luminosity for Pb-Pb collisions is given.

Table 2.1: The machine parameters relevant for the LHC detectors.[7]

At the LHC we are looking for extremely rare processes as is can be seen in figure 2.3 the production cross section of a SM Higgs boson is more than 9 orders of magnitude smaller than the total proton-proton cross section.

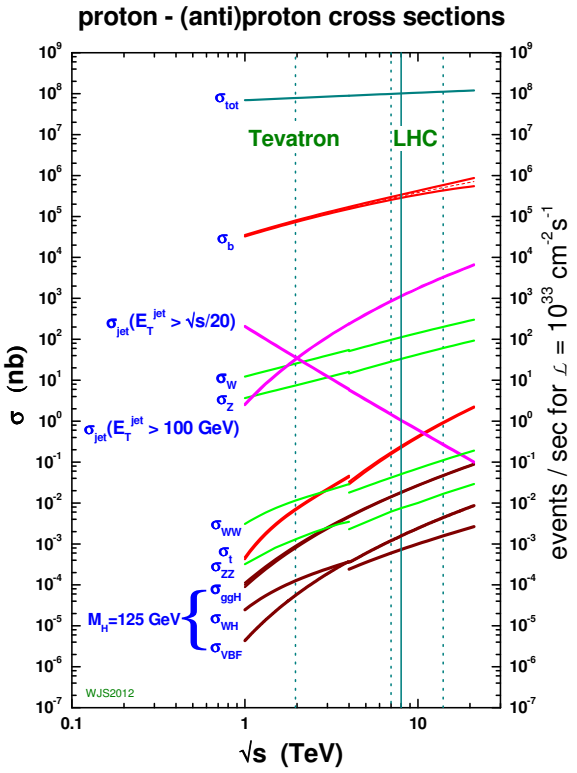

Figure 2.3: Cross sections for several processes for collisions of antiproton-proton and proton-proton as a function of the center of mass energy[4].

To be able to record and study such rare processes we need to produce a significant amount of collisions. For this purpose the LHC was designed to operate at high instantaneous luminosity, L. This quantity is defined as,

$$L = \frac{N_b^2 n_b f_{\text{rev}} \gamma}{4\pi \epsilon_n \beta^*} F, \tag{2.1}$$

where N_b is the number of protons per bunch, n_b is the number of bunches, f_{rev} is the frequency of revolution, γ is the Lorentz factor, ϵ_n is the normalized emittance, f_{rev} is the beta function at the collision point and F is the reduction factor due to the crossing angle.

2.1.1 Running and performance

The LHC has started its operation with the first circulation beams in September 2008. Unfortunately, only a few days after a faulty weld between two dipole magnets caused a significant magnet quench which in turn damaged several dipoles and a simultaneous leak of a significant amount of helium happened. The event showed that beyond the repair of the affected systems the accelerator needed a significant consolidation program to allow it to return to activity[8]. This consolidation program took over one year to finalise and to prevent further possible problems and allow better understanding of the machine while maximizing physics reach, it was decided to initially run the LHC at 7 TeV center-of-mass energy. First collisions happened at November 2009 just at the SPS injection energy of 450 GeV giving start to the LHC run I.

The collision energy was finally ramped up to 7 TeV with first collisions being observed during March 2010. Operation at this energy continued until the end of 2011, with the peak luminosity being achieved of $3.7 \times 10^{33} \mathrm{cm}^{-2}\mathrm{s}^{-1}$. The total amount of of integrated luminosity delivered to CMS was $6.1\,\mathrm{fb}^{-1}$ with the total actually recorded being $5.6\,\mathrm{fb}^{-1}$. During 2012 with the increase knowledge of the accelerator it was possible to increase the centre-of-mass energy further to 8 TeV and eventually reaching peak luminosity of $7.7 \times 10^{33}\,\mathrm{cm}^{-2}\mathrm{s}^{-2}$ and delivering $23.3\,\mathrm{fb}^{-1}$ to CMS of which $21.79, \mathrm{fb}^{-1}$ fb^{-1} were recorded. Figure 2.4 shows the delivered luminosity in the period 2010-2013 over time.

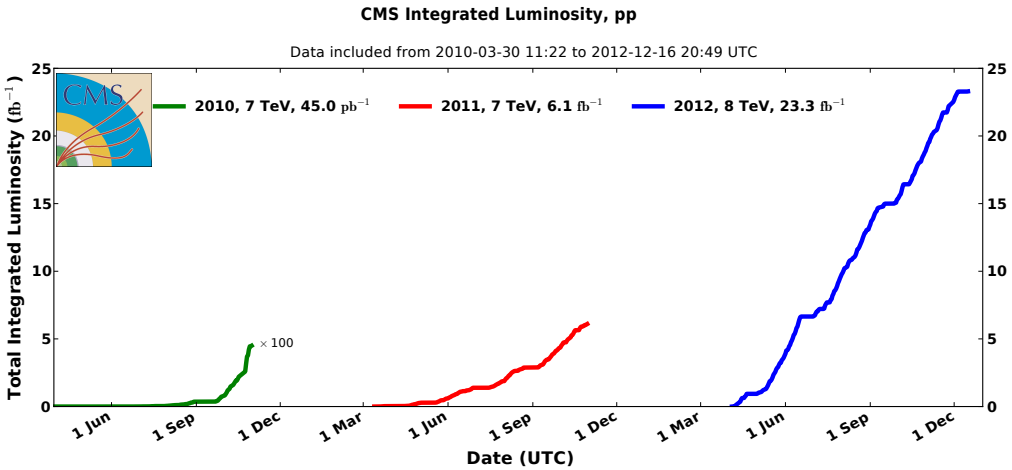

Figure 2.4: Cumulative luminosity versus day delivered to CMS during stable beams and for p-p collisions. This is shown for 2010 (green), 2011 (red) and 2012 (blue) data-taking.

For physics usage, data needs to undergo the process of certification. In this process specialists from each CMS subsystem check that no problem has happened during data

taking that would bias or invalidate the recorded events. For 2011 a total of $5.1\,\mathrm{fb}^{-1}$ and for 2012 a total $19.7\,\mathrm{fb}^{-1}$ were considered of good quality for physics.

In order to achieve high integrated luminosity LHC collides particle bunches 40 millions times a second, and many interactions may happen simultaneously, this effect is called Pile-Up (PU). A figure of the distribution of the mean number of interaction per bunch crossing during 2012 at the CMS experiment can be found in figure 2.5.

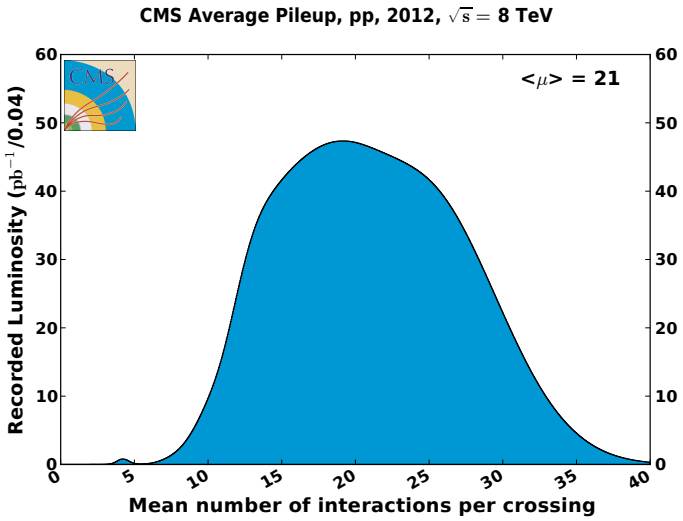

Figure 2.5: Mean number of interactions per bunch crossing at the CMS experiment during 2012.

2.2 The Compact Muon Solenoid Experiment

The experiment is a general purpose experiment located at the LHC point 5, near the village of Cessy, France. It was designed to be a high performance detector studying collisions at its centre. It is composed of several subsystems in a classic onion shaped structure. A diagram of the experiment can be found in figure 2.6.

The main driving motivation for its design is to investigate the electroweak symmetry breaking for which the Higgs mechanism at the design time was presumed to be the most likely explanation. Many other alternative theories to the standard model predict new particles which could be observed at the TeV scale, CMS as a multi-purpose experiment is well suited to search for this new scenarios. If found, such new physics may allow us to understand some of the currently open questions in particle physics, like providing a particle candidates for dark dark matter. Further more, some of this possible new

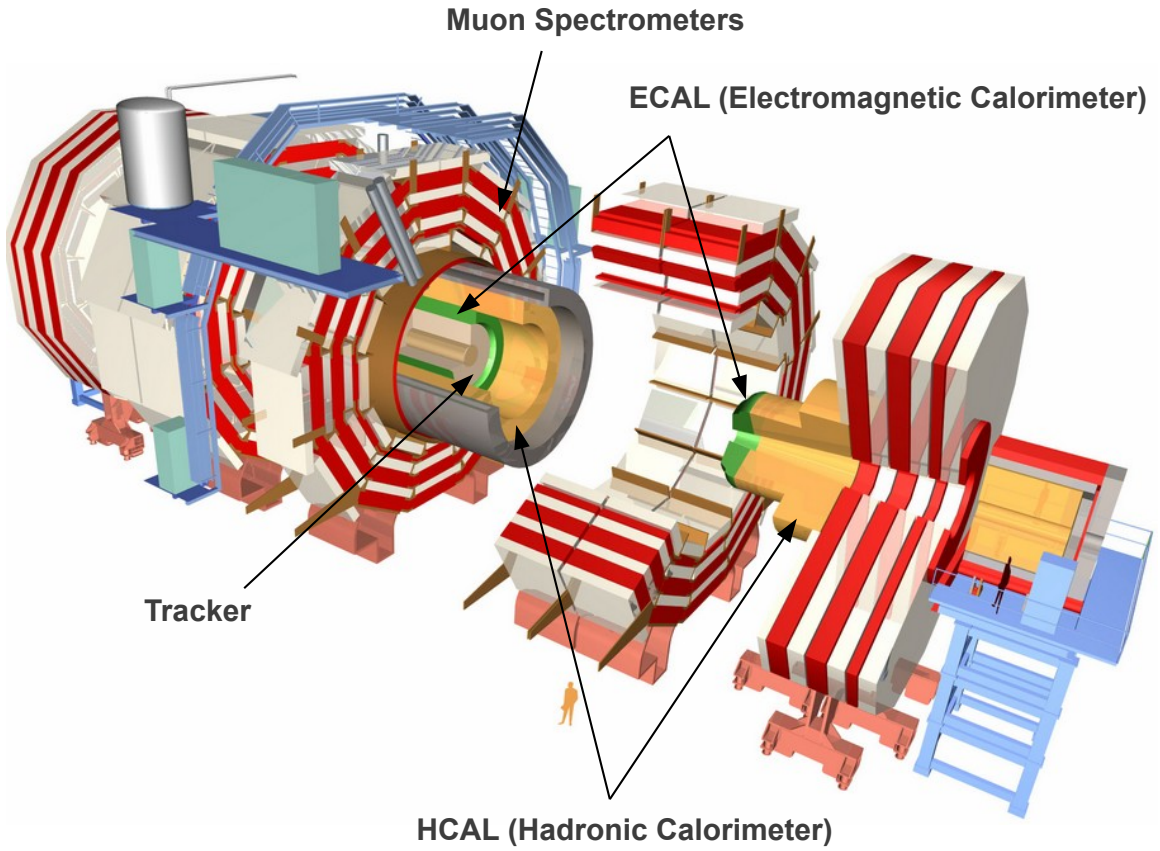

Figure 2.6: Diagram of Compact Muon Solenoid (CMS) experiment showing the experiment in an open configuration and highlighting the position of its sub-detectors.

physics signals could point the way towards a grand unified theory. CMS is also capable of operating while the LHC is colliding heavy ions and has a rich program covering the study of Quantum Chromodynamics (QCD) matter at extreme temperatures, density and parton momentum fraction (low-x).

The requirements imposed to CMS design to meet its physics goals can be summarized in the following table[4]:

- Good muon identification and momentum resolution over a wide range of momenta and angles, good dimuon mass resolution ($\approx 1\%$ at $100\,GeV$), and the ability to determine un-ambiguously the charge of muons with $p_{\mathrm{T}} < 1\,\mathrm{TeV}$.
- Good charged-particle momentum resolution and reconstruction efficiency in the inner tracker. Efficient triggering and offline tagging of τ's and b-jets, requiring pixel detectors close to the interaction region.

- Good electromagnetic energy resolution, good diphoton and dielectron mass resolution ($\approx 1\%$ at 100 GeV), wide geometric coverage, π^0 rejection, and efficient photon and lepton isolation at high luminosities.
- Good missing-transverse-energy and dijet-mass resolution, requiring hadron calorimeters with with a large hermetic geometric coverage and with fine lateral segmentation.

The final detector design fulfils all this requirements. The experiment is compact compared with the other LHC experiments being 22 m long and 15 m in diameter. Although small, it is the heaviest of the four big detectors at 12500 t. Its high density is a direct consequence of it producing the highest magnetic field at 4 T and therefore needing more material for it to be contain in its return yoke. On the next section we will go in detail over the features and technologies used.

2.2.1 Geometry and conventions

The adopted coordinate system has it origin in the center of CMS where the nominal collision point is located, the y-axis points vertically upwards, and the x-axis points radially inward in the direction of the centre of the LHC. The z-axis points along the beam line towards the Jura mountains from the LHC point 5. The azimuthal angle ϕ is measured from the x-axis in the x-y plane. The polar angle θ is measured from the z-axis.

We define pseudorapidity as $\eta = -ln(tan(\theta/2))$. All transverse quantities, like the transverse momentum ($p_\perp$), are measured in the transverse plane of beam axis. The imbalance of energy is also measured in the x-y plane and is denoted as $E_\perp^{miss}$.

2.2.2 Inner tracking system

The inner tracking system is the closest detector to the beam axis and the interaction region. Its function is to measure the trajectory of all charged particles, like electrons, charged hadrons and muons with momentum above 1 GeV being produced at each LHC collision. With the help of the strong magnetic field produced by the CMS magnet, particle trajectories are bent allowing for charge and momentum determination. With the resulting tracks is it then possible to determine the primary vertex as well as secondary vertexes like other lower energy proton-proton collision or displaced vertexes from the decay of long lived particles like B mesons.

Building a tracking system for an experiment at the LHC is very challenging. At design luminosity an average of 1000 particles will hit such system at a rate approaching 40 MHz, leading to high hit density at high rate. It is therefore desirable to have a fast, efficient and high granularity detector. Where at each layer the occupancy should be at or below 1%. On the other hand each layer should be as thin as possible in order to not change the incoming particles trajectory or make them lose too much energy. The detector should also be radiation hard and survive for a period of at least 10 years due to its importance and location. This design requirements have lead to a tracker design entirely based on silicon detector technology.

The volume near the interaction point can be split according to the charged particle flux into three regions:

- $r < 10\,\text{cm}$: highest particle flux, up to $\approx 10^8 \text{cm}^{-2}\text{s}^{-1}$ at $r \approx 4\text{cm}$, pixel detectors are used. The pixel size is $\approx 100 \times 150\,\mu\text{m}^2$, which translates into an occupancy of 10^{-4} per LHC bunch crossing.
- $20 < r < 55\,\text{cm}$: particle flux decreases enough to use silicon micro-strips with a minimum cell size of $10\,\text{cm} \times 80\,\mu\text{m}$, leading to an occupancy of $\approx 2 - 3\%$ per LHC bunch crossing.
- $50 < r < 110\,\text{cm}$: most outer region of the tracker, particle flux is low enough to use larger pitch silicon micro-strips. The maximum cell size is of $25\,\text{cm} \times 180\,\mu\text{m}$, and occupancy is of the order of $\approx 1\%$.

The CMS tracker final configuration is composed of a pixel detector with three barrel layers at radii between 4.4 cm and 10.2 cm and 2 disks on each side of the barrel. And a silicon strip tracker with 10 barrel detection layers extending up to 1.1 m with 3 plus 9 disks on each side of the barrel. A schematic of this detector module distribution can be found at figure 2.7. This detector has an acceptance covering up to pseudorapidity of $|\eta| < 2.5$ and has a total active area of about $200\,\text{m}^2$ making the largest silicon tracker ever built.

2.2.3 Electromagnetic Calorimeter

The Electromagnetic Calorimeter (ECAL) is the detector responsible for measuring the energy of electrons and photons. It is an hermetic energy measurement system comprised of 61200 lead tungstate ($PbWO_4$) crystals mounted in the barrel and 7324 crystals in each of the 2 endcaps and it has an acceptance up to $|\eta| < 3.0$.

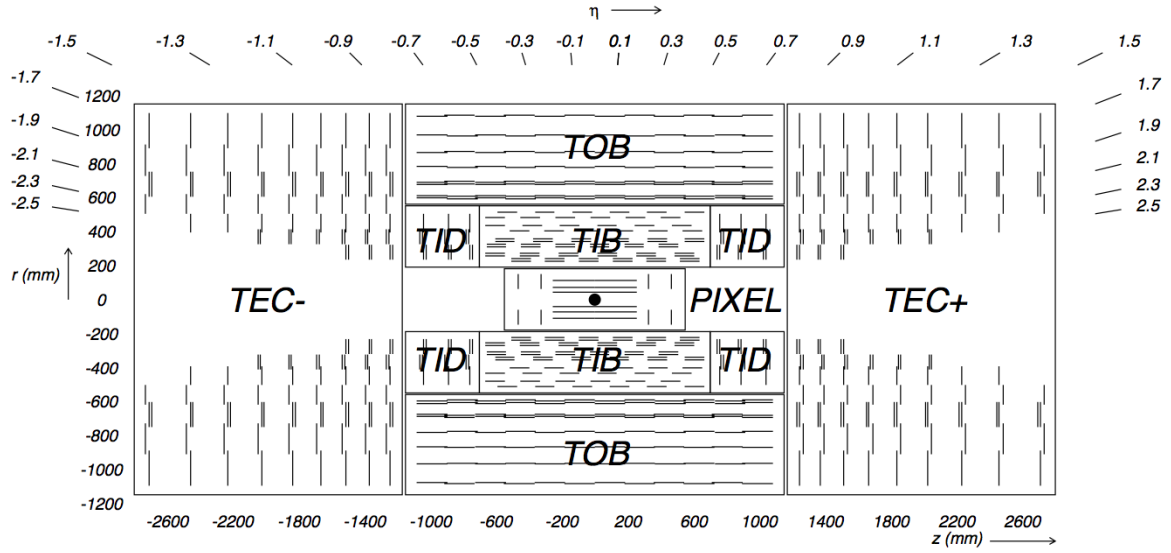

Figure 2.7: Schematic cross section of the CMS tracker. Each line represent a detector module. Double lines represent dual surface back-to-back detector modules.

Lead tungstate has a fairly high density (8.28 g/cm^3), has a short radiation length (0.89 cm) and a small Moliere redius (2.2 cm). The crystals also have a fast scintillation decay time emitting 80% of the light yield in 25 ns (the minimal bunch crossing time at the LHC). This characteristics make it a good choice for an electromagnetic calorimeter allowing a compact design with fine granularity. However, this crystals emit a fairly low light yield (30 γ/MeV) which requires the use of photo-detectors with intrinsic gain which will preform well inside a magnitic field. In the barrel region silicon Avalanche photo-diodes (APD) are used and Vacuum Photo-Triodes (VPT) are used in the endcaps. To guarantee good response from both crystals and APD it is necessary to have system thermal stability, with the goal being temperature variation of less than 0.1°C.

The barrel section, the ECAL Barrel (EB), has an inner radius of 129 cm and is composed of 36 identical "supermodules", each covers the barrel length and corresponding to a pseudo-rapidity interval of $0 < |\eta| < 1.479$. The crystals are quasi-projective (the axes are tilted at 3° with respect to the line from the nominal vertex position) and cover 0.0174 (i.e. 1°) in $\Delta\phi$ and $\Delta\eta$. The crystals have a front face cross-section of $\approx 22 \times 22\,\text{mm}^2$ and a length of 230 mm, corresponding to 25.8 X_0.

The endcap section, the ECAL Endcap (EE), is at a distance of 314 cm from the vertex and covering a pseudorapidity range of $1.479 < |\eta| < 3.0$, are each structured as 2 "Dees", consisting of semi-circular aluminium plates from which are cantilevered structural units

of 5×5 crystals, known as "supercrystals". A diagram of the ECAL can be found on figure 2.8.

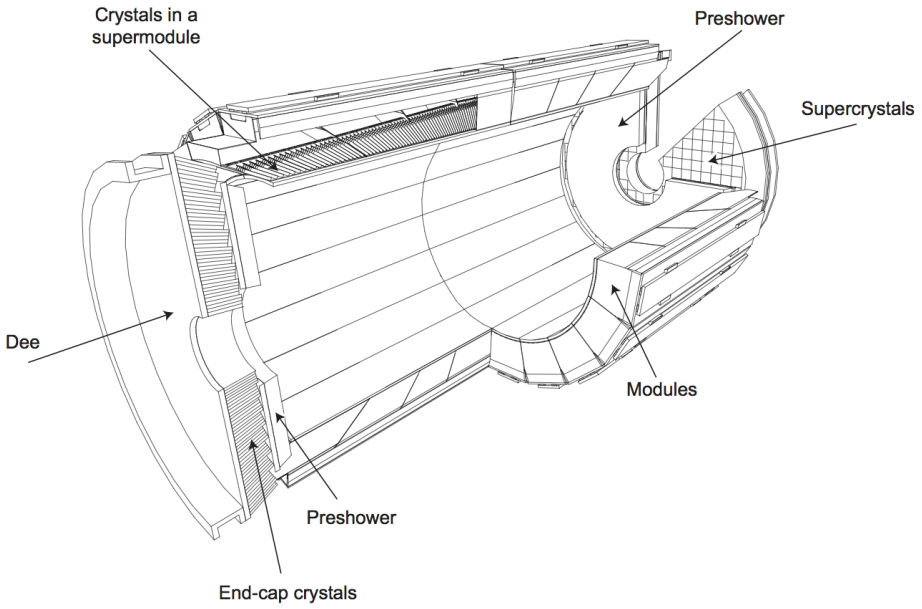

Figure 2.8: Diagram of the ECAL layout illustrating the positions of its components.

The energy resolution of the ECAL can be can be expressed as:

$$\frac{\sigma}{E} = \frac{S}{\sqrt{E}} \oplus \frac{N}{E} \oplus C \tag{2.2}$$

Here E is the energy of the incoming particle, S is the stochastic term which quantifies the fluctuations in scintillation and lateral containment of the shower, N the noise term which relates with electronics and digitisation process and finally C is a constant term that quantifies the non-uniform longitudinal response and inter-calibration errors. These parameters have been measured to be $S = 0.028\,\mathrm{GeV}^{1/2}$, $N = 0.12\,\mathrm{GeV}$ and $C = 0.003$ with the help of an electron beam[9] and in the absence of magnetic field.

2.2.4 Hadronic Calorimeter

The is a sampling calorimeter which is designed to measure the properties of hadron jets and indirectly neutrinos or other undiscovered particles that would result in apparent missing energy[10]. The design of the Hadronic Calorimeter (HCAL) was strongly

influenced by the choice of the magnet parameters since most of the calorimetry is inside of the magnet. A diagram of the HCAL subsystems and their location inside CMS can be found in figure 2.9.

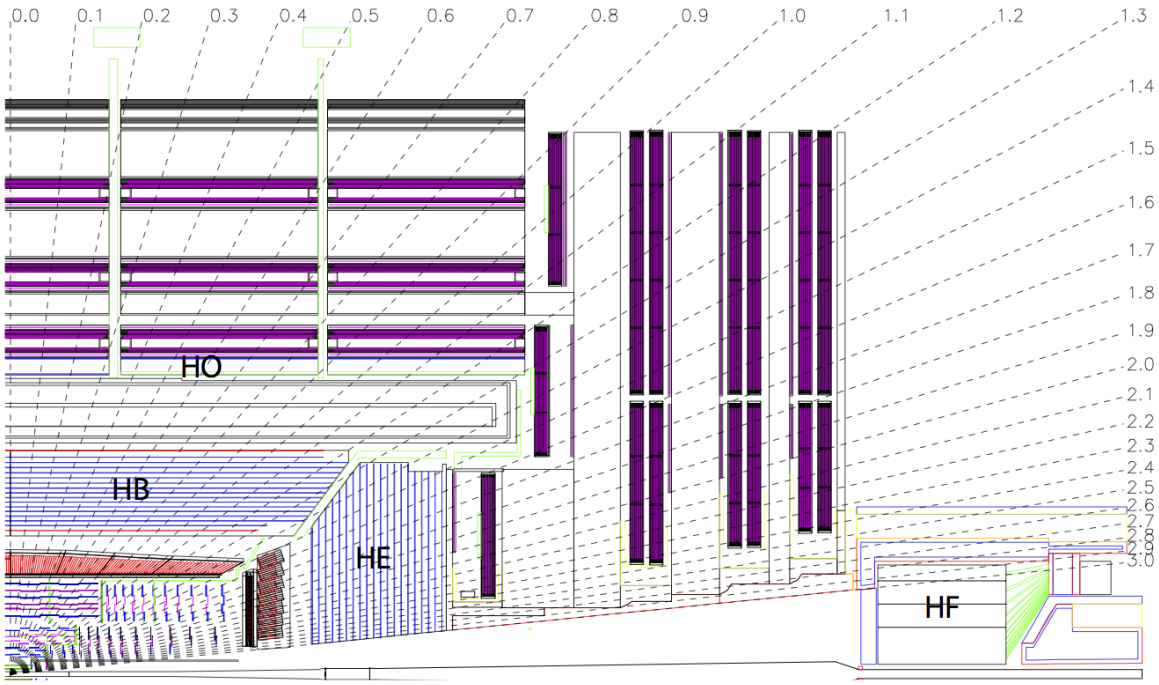

Figure 2.9: Longitudinal view of the CMS detector highlighting the location of the HCAL components: HCAL Barrel (HB), HCAL Endcap (HE) HCAL Outer (HO) and HCAL Forward (HF).

The covers the region up to $|\eta| < 1.3$ and is limited from the beam side by the ECAL at radius $r = 1.77\,\text{m}$ and outwards by the magnet at radius $r = 2.95\,\text{m}$. This is a strict limitation on the amount of absorber material to be used. This detector is composed of 36 identical azimuthal wedges split in two half-barrels. They are constructed of brass absorber plates alternated with plastic scintillator. Brass has a short interaction length ($X_0 = 16.42\,\text{cm}$) and is non-magnetic. The detector is composed of 2304 towers with a segmentation of $\Delta\eta \times \Delta\phi = 0.087 \times 0.087$ which corresponds to the same area of a 5×5 arrays of ECAL crystals.

To improve the measurement capability, an outer calorimeter, the , is placed outside of the magnet as a *tail catcher*. It increases the effective thickness of the hadronic calorimeter by over 10 interaction lengths. This detector covers the range $|\eta| < 1.26$, it is composed or iron absorber and scintillator and is subdivided into sectors that cover 30^{o} azimuthal angle in each of the barrel wheels.

The covers the range of $1.3 < |\eta| < 3.0$. It is composed by 2034 towers with a 14 towers segmentation in η and 5° segmentation in ϕ. The 8 inner most towers the segmentation is 10° in ϕ, whilst the η segmentation increases in η from 0.09 to 0.35.

Additionally, to extend acceptance to $|\eta| < 5.2$ the HF is installed at 11.2 m from the interaction point providing excellent hermeticity for $E_{\perp}^{miss}$ measurement. Its steel absorber is 1.65 m deep and has quartz fibres running through it, parallel to the beam line. The energy measurement is made via Cerenkov light produced by the incoming particles inside the fibres. There are 13 tower in η with segmentation of $\approx \Delta\eta = 0.175$ except the lowest η tower with $\approx \Delta\eta = 0.1$ and highest η tower with $\approx \Delta\eta = 0.3$. The segmentation in ϕ is of $\Delta\phi = 10°$ except in the highest η towers which is $\Delta\phi = 20°$. There are a total of tower 900 per HF module.

Similarly to the ECAL the energy resolution HCAL was tested using a test beam of single charged pions[9], and it was obtained that:

$$\frac{\sigma}{E} = \frac{94.3\%}{\sqrt{E}} \oplus 8.4\%. \tag{2.3}$$

2.2.5 Solenoid Magnet

The design requirements for correct charge assignment and p_{T} determination for charge particles and specially muons drive the magnet parameters choice. For muons, unambiguously charge determination requires momentum resolution of $\Delta p/p \approx 10\%$ at $p = 1\mathrm{TeV}$. This requirements are specially difficult to obtain in the forward regions but with the correct length/radius ratio can be obtained with a modestly sized solenoid magnet but with large field[11].

The choice of the CMS collaboration was to build a Niobium-Titanium (NbTi) superconducting solenoid magnet which has been design to operate at fields up to 4 T it has a diameter of 6 m and a length of 12.5 m at maximum field the stored energy reaches 2.7 GJ. Typically, the magnet is only run at 3.8 T in order to maximize its lifetime. To contain such an enormous magnetic flux a 10 kt return yoke envelopes the magnet with 5 wheels in the barrel region and 2 endcaps composed of 3 disks closing the sides[4]. A summary of the most important magnet parameters can be found at table 2.2.

Parameter	Value
Field	4 T
Inner Bore	5.9 m
Length	12.9 m
Number of turns	2168
Current	19.5 kA
Stored Energy	2.7 GJ
Hoop Stress	64 atm

Table 2.2: Parameters of the CMS superconducting solenoid

2.2.6 Muon System

The muon detection is an important part of the mission of CMS as the middle name of the experiment indicates. Muons are fairly easy to detect when compared with other elementary particles and are only rarely produced in proton-proton collisions. Lets take the example of the SM Higgs boson, while the decay mode involving a pair of Z bosons is fairly unlikely compared with other decays the Z bosons can decay into 4 mouns. This decay while rare does not have significant backgrounds making it a "golden channel" for discovery, which indeed was proven the case[12]. Many other models, like SUSY, use muon final states in their searches exactly for the same reason. The CMS muon system is composed of 3 types of gaseous detectors depending on they location and momentum reconstruction needs. A diagram of the disposition of this system inside CMS can be found on figure 2.10.

In the barrel and up to $|\eta| < 1.2$, Drift Tube (DT) are used. since the neutron background is small and the field is constant. This system is composed 250 chambers and is arranged in 4 concentric cylindrical layers which are installed inside of the return yoke. This chambers have a total of 172000 wires with a length of 2.4 m which are housed inside of tubes filled with a mixture of argon and carbon-dioxide. Each of the wheels of the barrel is split into 12 sectors covering 30° azimuthal angle. The maximum gas ionization drift is of 2.0 cm and results in a single point resolution is $\approx 200\,\mu$m per wire. For each station each measured muon the ϕ resolution is better than 200 µm and direction resolution is ≈ 1 mrad.

In the endcaps Cathode Strip Chamber (CSC) are used in the region between $2.4 > |\eta| > 0.9$. Here, muon and background rates are high and the magnetic field is not uniform. This system has fast response and is radiation resistant. It is composed by 468 chambers

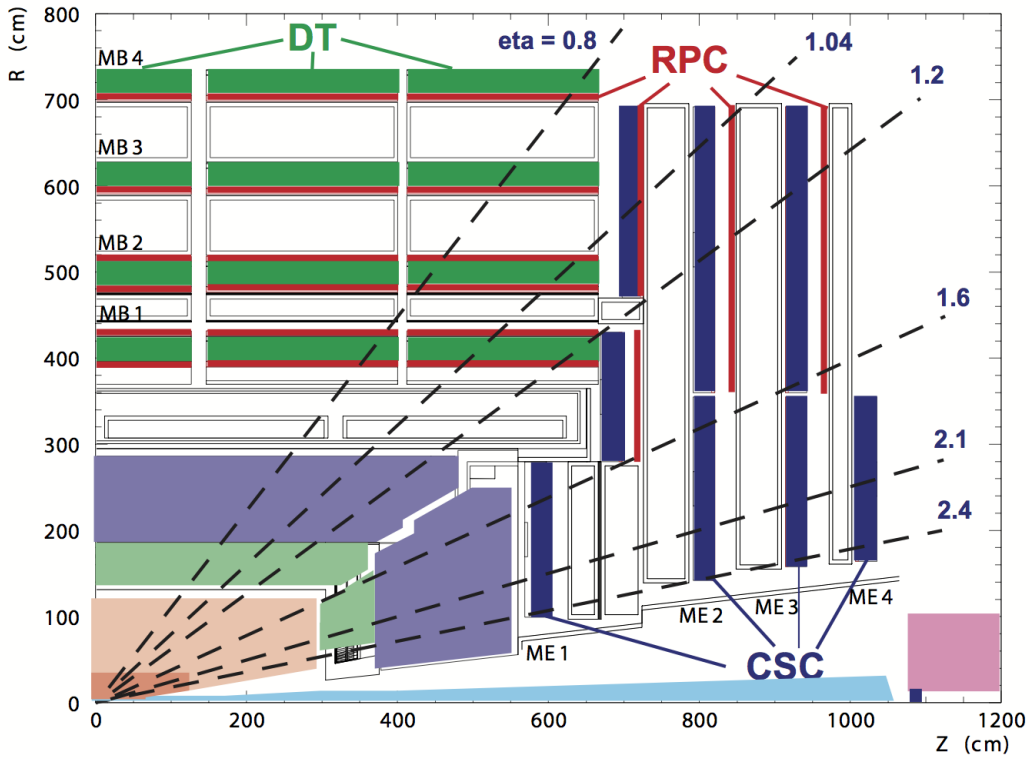

Figure 2.10: Diagram of the CMS muon systems. The location of each muon chamber for each subsystem is showed.

arranged in 4 stations per side. Each chamber is trapezoidal in shape and made of 6 gas gaps and covers either 10° or 20° in ϕ. Each gap contains a plane of cathode strips and a plane of anode wires. For each chamber the spacial resolution is of the order of 200 µm and the angular resolution is ≈ 10 mrad in ϕ.

Finally the Resistive Plate Chamber (RPC) covers the $|\eta| < 1.6$ range. This system overlaps with the 2 other muon systems. It is very fast with an ionization event being much faster than the bunch crossing time. This fast response allows, in conjunction with a dedicated trigger system, to select the correct bunch crossing associated with the detection of a muon. In the barrel there 480 rectangular chambers arranged in 4 stations with 6 RPC layers (2 layers are present in the 2 stations closest to the beam pipe). In the endcaps there are 3 RPC disk shaped stations on each side, which are composed by trapezoidal shaped detectors.

The combined muon system offline momentum resolution is of the order of 9% for small values of η and p and for transverse momenta of up to 200 GeV. At higher energies of around 1 TeV the standalone momentum resolution is in the range of 15-40% depending on $|\eta|$. This values are limited by the muon multiple-scattering before arriving to the

muon system. If we combine the tracker information into a global fit the resolution for lower p_T tracks improves an order of magnitude while at higher momenta (around 1 TeV) it is of about 5%, which is well inside the CMS design requirements.

2.2.7 Data Acquisition System

The CMS Data Acquisition (DAQ) system is designed to process, analyse and ultimately store the information collected by the detector. The LHC produces bunch crossings at a rate of 40 MHz but we are only capable of storing between $10^2 - 10^3$ events per second. At design luminosity each collision will have an average of 20 simultaneous collisions and produce a zero-suppressed data payload of around 1 MByte. To reduce the initial event rate a first level of trigger was designed in order to reduce the amount of events to be processed to a maximum of 100kHz. Even with this event suppression the DAQ has to handle $\approx$ 100GBytes^{-1} which come from approximately 650 data sources. The information is collected and passed to a computer farm where a software filters serve as a second level of trigger, this system is known as the . In this system the event rate is further reduced by a factor of 1000 making the output rate compatible with what can be saved into permanent storage. A diagram of this system can be found on figure 2.11.

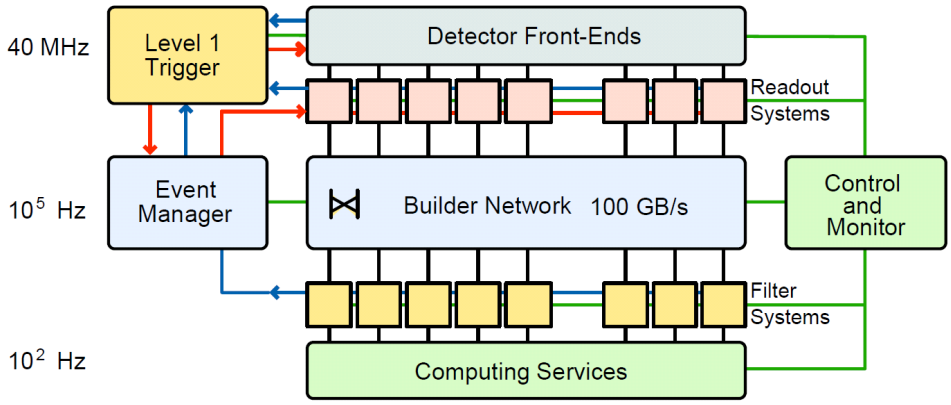

Figure 2.11: Diagram of the CMS DAQ system. Data flow is showed as the lines connecting each electronics or computing units.

2.2.8 Trigger System

At the nominal LHC running conditions the luminosity will be of the order of $10^{34}\,\mathrm{cm}^{-2}\mathrm{s}^{-1}$ where 20 simultaneous collisions will happen at a rate of 40 MHz spaced only by 25 nm.

This means we have every second 10^9 interaction. We can only save $10^2 - 10^3$ events per second with our computer systems. This implies that our trigger system needs to obtain a data reduction of a factor of $10^6 - 10^7$. This is achieved with a two level trigger system, the first is a dedicated hardware system named and the second is a commercial computer system running dedicated software called the [13].

Initially, all data is stored for 128 bunch crossing which corresponds to 3.2 µs. This is the time we have to make a first decision to keep or discard each event. This is the task of the Level 1 Trigger (L1T) which has the target to reduced the data to a maximum rate of 100 kHz. In the allocated time there isn't enough time to get all the information from the detector, so only a coarse version of the calorimetry and muon systems data and some correlation between them is accessed. With this information the L1T produces a set of particle candidates and energy sums over which custom user defined algorithm can filter the events. A diagram of the L1T trigger components and the data flow across the system is present on figure 2.12.

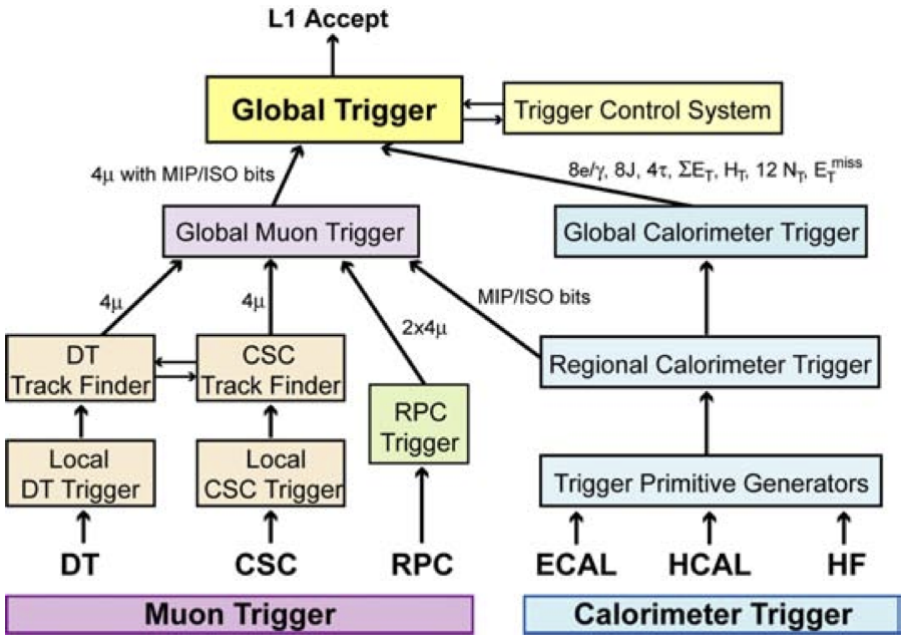

Figure 2.12: Diagram of the L1T system. The arrows indicate data flow and the number of particle candidates at each step is indicate.

The High Level Trigger (HLT) receives events from the L1T and needs to preform further event reduction of $\mathcal{O}(10^5)$ to a final output rate of $\mathcal{O}(10^{2-3})$ Hz . This system is composed of standard computing hardware in the form of computing farm with several thousands of Central Processing Unit (CPU). This system, using the additional latency created by the

L1T event selection, is able to make use of the complete detector information including the tracker data. More sophisticated and precise algorithms are therefore possible which can be tailored to select any desired physical final state.

Both event selection algorithms at the L1T and HLT are constantly updated during data taking. Many times it is necessary to update the selection thresholds in order to control the rate with the increase of LHC luminosity, but such changes can also be due to the development of novel methods or strategies to identify particles more efficiently or the interest in recording new event final final states. The set of algorithms used for data taking is normally referred as the *trigger menu*.

After events passing both levels of the trigger they are recorded into permanent storage. During 2012-13 operation two output streams were saved. The *prompt data stream*, with a rate of approximately 300 Hz, was composed of high priority trigger paths which were immediately reconstructed. And the *parked data stream*, with a rate up to 1 kHz, was stored without reconstruction. This data waited until computing resources would be free to go through reconstruction[14]. This process was finalised a few months after the LHC run I was finished.

Even with such measures to reduce the data to be stored, each LHC experiment records several petabytes of data every year in addition to similarly sized amounts of simulated events.

2.2.9 Computing

The quantity of data produced by LHC and the processing necessary are so big that it would be difficult to have all computing resources in a single place. For this reason a tiered system was developed, where all participating computing sites are connected and have specific roles and responsibilities in the data taking, processing and storing.

The CERN Data Centre is the Tier 0 of this network, know as the Grid. All data produced by the LHC passes through it. Only about 20% of the total capacity of the Grid is hosted here, but CERN has the very important mission of safe keeping all the raw data produced by the LHC experiments. It also has the task of doing the first attempt at reconstructing this data into meaningful physics objects.

There are 13 Tier 1 computer centres around the world. They are responsible to store a proportional amount of raw and reconstructed data among them. If any reprocessing of the data is needed, this centres are responsible for this task and storing the resulting

output as well. Tier 1 centres also host simulated data and distributing it to affiliated Tier 2 centres.

Local research centres like universities of scientific laboratories are normally at the Tier 2 level. They should have enough computing power and storage space for the analysis in which those centres are involved. This centres will have the responsibility of handling a proportional share of simulated data production and reconstruction. Currently there are over 150 tier 2 centres around the world

Individual computers or local clusters without any formal engagement with the Grid structure, are at considered to be the Tier 3 level of the Grid.

2.2.10 Level 1 Trigger: Stage I Upgrade

An extensive upgrade program for the L1T electronics was planed and is being executed in order to cope with the increase of luminosity and pile-up predicted for the period after Long Shutdown 1 (LS1)[15]. It is expected that center-of-mass energy will almost double from 8 TeV to 13 TeV, instantaneous luminosity will also increase as will average pile-up. Also, the bunch separation with change from 50 ns to 25 ns making out-of-time pile-up a significant problem.

To ensure physics performance during 2015 only a partial upgrade is planned which is known as the *Stage-1* upgrade. The main feature of this upgrade is the replacement of the existing Global Calorimeter Trigger (GCT). Two key enhancements will be possible from the upgrade:

- Event-by-event pile-up energy subtraction for jets reconstruction, e/γ isolation, τ isolation.
- Smaller feature size τ candidates, which will have significantly better energy estimation and background rejection.

The intermediate system will have significantly better performance than the now legacy system. The full 2016 calorimeter trigger system will additionally provide finer granularity which will lead to increased position and energy resolution.

Chapter 3

Technical work

3.1 Level 1 Trigger Data Quality Monitoring System

Hello

Chapter 4

Physics Objects and Monte Carlo simulation

4.1 Physics objects definition

4.1.1 Electron

4.1.2 Muon

4.1.3 Tau

4.1.4 Jets

4.1.5 Missing Transverse Energy

4.2 Monte Carlo simulation

Chapter 5

Prompt Data Analysis

Chapter 6

Parked Data Analysis

Chapter 7

Run II Preparation

7.1 Run II trigger studies

7.2 Run II QCD Monte Carlo samples

Chapter 8

Conclusions

Summary of relevant results and their impact on Particle Physics

Bibliography

[1] L. Evans and P. Bryant, "LHC Machine", *JINST* **3** (2008) S08001, doi:10.1088/1748-0221/3/08/S08001.

[2] LEP Injector Study Group Collaboration, "LEP Design Report, Volume 1: The LEP Injector Chain",.

[3] ATLAS Collaboration, "The ATLAS Experiment at the CERN Large Hadron Collider", *Journal of Instrumentation* **3** (2008), no. 08, S08003.

[4] CMS Collaboration, "The CMS experiment at the CERN LHC", *Journal of Instrumentation* **3** (2008), no. 08, S08004.

[5] LHCb Collaboration, "The LHCb Detector at the LHC", *Journal of Instrumentation* **3** (2008), no. 08, S08005.

[6] ALICE Collaboration, "The ALICE experiment at the CERN LHC", *Journal of Instrumentation* **3** (2008), no. 08, S08002.

[7] CMS Collaboration, "CMS Physics: Technical Design Report Volume 1: Detector Performance and Software", technical report, Geneva, (2006). There is an error on cover due to a technical problem for some items.

[8] M. Bajko, F. Bertinelli, N. Catalan Lasheras et al., "Report of the task force on the incident of 19th September 2008 at the LHC", *LHC Project Report* **LHC-PROJECT-REPORT-1168** (2009).

[9] USCMS, ECAL/HCAL Collaboration, "The CMS barrel calorimeter response to particle beams from 2-GeV/c to 350-GeV/c", *Eur. Phys. J.* **C60** (2009) 359–373, doi:10.1140/epjc/s10052-009-0959-5,10.1140/epjc/s10052-009-1024-0. [Erratum: Eur. Phys. J.C61,353(2009)].

[10] CMS Collaboration, "CMS, the Compact Muon Solenoid: Technical proposal",.

[11] C. Collaboration, "Technical proposal for the upgrade of the CMS detector through 2020", Technical Report CERN-LHCC-2011-006. LHCC-P-004, CERN, Geneva, (Jun, 2011).

[12] CMS Collaboration, "Observation of a new boson at a mass of 125 GeV with the CMS experiment at the LHC", *Phys. Lett.* **B716** (2013) 30–61, doi:10.1016/j.physletb.2012.08.021, arXiv:1207.7235.

[13] CMS Collaboration, "CMS. The TriDAS project. Technical design report, vol. 1: The trigger systems",.

[14] CMS Collaboration Collaboration, "Data Parking and Data Scouting at the CMS Experiment",.

[15] CMS Collaboration, "CMS Technical Design Report for the Level-1 Trigger Upgrade",.

List of Figures

2.1 Underground diagram of the Geneva area showing the LHC and its experiments location. . . . 4
2.2 Diagram of the CERN accelerator complex. . . . 6
2.3 Cross sections for several processes for collisions of antiproton-proton and proton-proton as a function of the center of mass energy[4]. . . . 7
2.4 Cumulative luminosity versus day delivered to CMS during stable beams and for p-p collisions. This is shown for 2010 (green), 2011 (red) and 2012 (blue) data-taking. . . . 8
2.5 Mean number of interactions per bunch crossing at the CMS experiment during 2012. . . . 9
2.6 Diagram of CMS experiment showing the experiment in an open configuration and highlighting the position of its sub-detectors. . . . 10
2.7 Schematic cross section of the CMS tracker. Each line represent a detector module. Double lines represent dual surface back-to-back detector modules. 13
2.8 Diagram of the ECAL layout illustrating the positions of its components. 14
2.9 Longitudinal view of the CMS detector highlighting the location of the HCAL components: HCAL Barrel (HB), HCAL Endcap (HE) HCAL Outer (HO) and HF. . . . 15
2.10 Diagram of the CMS muon systems. The location of each muon chamber for each subsystem is showed. . . . 18
2.11 Diagram of the CMS DAQ system. Data flow is showed as the lines connecting each electronics or computing units. . . . 19
2.12 Diagram of the L1T system. The arrows indicate data flow and the number of particle candidates at each step is indicate. . . . 20

List of Tables

1.1 List of leptons and their fundamental properties 2
1.2 List of quarks and their fundamental properties 3
1.3 List of bosons and their fundamental properties 3

2.1 LHC parameters relevant for detectors 6
2.2 Parameters of the CMS superconducting solenoid 17

Acronyms

ALICE A Large Ion Collider Experiment. 5

APD Avalanche photo-diodes. 13

ATLAS A Toroidal LHC ApparatuS. 5

BSM Beyond the Standard Model. 5

CERN European Organization for Nuclear Research. 4–6, 21, 32

CMS Compact Muon Solenoid. 5, 8–12, 15–19, 32

CPU Central Processing Unit. 20

CSC Cathode Strip Chamber. 17

DAQ Data Acquisition. 19, 32

DT Drift Tube. 17

EB ECAL Barrel. 13

ECAL Electromagnetic Calorimeter. 12, 14–16

EE ECAL Endcap. 13

FCT Fundação para a Ciência e a Tecnologia. vi

GCT Global Calorimeter Trigger. 22

HB HCAL Barrel. 15, 32

HCAL Hadronic Calorimeter. 14–16, 32

HE HCAL Endcap. 15, 32

HF HCAL Forward. 15, 16, 32

HLT High Level Trigger. 20, 21

HO HCAL Outer. 15, 32

L1T Level 1 Trigger. 20–22, 32

LEP Large Electron Positron collider. 4

LHC Large Hadron Collider. 4–13, 19, 21, 32

LHCb Large Hadron Collider beauty. 5

LINAC2 Linear Particle Accelerator 2. 5

LS1 Long Shutdown 1. 22

PS Proton Synchrotron. 5

PSB Proton Synchrotron Booster. 5

PU Pile-Up. 9

QCD Quantum Chromodynamics. 10

RF Radio Frequency. 6

RPC Resistive Plate Chamber. 18

SM Standard Model. 2, 7, 17

SPS Super Proton Synchrotron. 5, 8

VPT Vacuum Photo-Triodes. 13